Optical study of the multiple charge-density-wave transitions in ErTe₃

B. F. Hu, B. Cheng, R. H. Yuan, T. Dong, A. F. Fang, W. T. Guo, Z. G. Chen, P. Zheng, Y. G. Shi, and N. L. Wang

Beijing National Laboratory for Condensed Matter Physics, Institute of Physics, Chinese Academy of Sciences,
Beijing 100190, People's Republic of China

We present an optical spectroscopy study on singe crystalline ErTe₃, a rare-earth-element tritelluride, which experiences two successive charge-density wave (CDW) transitions at $T_{c1} = 267$ K and $T_{c2} = 150$ K. Two corresponding gap features, centered at 2770 cm^{-1} ($\sim$343 meV) and 890 cm^{-1} ($\sim$110 meV), respectively, are clearly seen in ordered state. A pronounced Drude component, which exists at all measurement temperatures, demonstrates the partial gap character of both CDW orders. About half of the unmodulated Fermi surface (FS) remains in the CDW state at the lowest measurement temperature. The study also indicates that fluctuation effect may be still prominent in this two-dimensional material.

I. INTRODUCTION

Charge-density waves (CDWs), as typical broken-symmetry states in solids,[1] have received considerable attention in the past decades. To date, the CDW orders are accepted to be predominantly driven by the nesting of the metallic Fermi surfaces (FSs). Such nesting would cause a divergence of the electronic susceptibility and response function at the nesting wave vector $\mathbf{k}_F$, resulting in instability of the FS. An energy gap in the single-particle excitation spectrum would open near the Fermi level, leading to lowering of the total energy of the system. In real space, the instability would result in a spatially periodical modulation of charge density distribution $\rho(\mathbf{r})$ with a period of $\lambda = \pi/\mathbf{k}_F$. Mediated by the electron-phonon coupling, it also causes a displacement or superstructure distortion of the underlying lattice. Up to now, a great deal of experimental and theoretical investigations have been done aiming at exploring and understanding the intriguing collective quantum phenomena in a variety of CDW materials. The low-dimensional systems that have a highly anisotropic crystal structure are especially concerned due to the relatively easy realization of the FS nesting condition. Nevertheless, except for the one-dimensional electron system, perfect nestings among the entire FS could hardly be achieved in real materials. More often, only parts of the FS are nested that could be connected by a wave vector that matches with a peculiar phonon anomaly. In this circumstance, only a partial energy gap opens on the FS in the optimally nested area and some metallic channels are saved in the ordered state.

The discovery of the CDW character in the rare-earth tritelluride RTe₃ ($R =$ Y, La, and rare-earth elements) systems[2] has provided an ideal opportunity to probe the CDW properties, which have been well characterized by the FS-nesting-driven mechanism.[3–8] RTe₃ has a layered, weakly orthorhombic crystal structure (No. 63 space group *Cmcm*),[9,10] making up of two nearly square Te nets, which are separated by an insulating corrugated RTe slab. The former undertakes the metallic conductive task, while the latter plays a role of charge reservoirs.[5,10] The lattice of the compounds has an incommensurate modulation with a wave vector of approximately $2/7c^*$ in the CDW state.[2] The transition temperature decreases monotonically on traversing the lanthanides series from the lighter rare-earth to the heavier ones,[11–13] which

is slightly below the room temperature for the heavy rare-earth RTe₃[11] but believed to be even above the melting point for the first several light rare-earth compounds.[4] An angle-resolved photoemission spectroscopy (ARPES) study has well demonstrated the evolution of the CDW properties,[7] including the effect of chemical pressure on the energy gaps and the distribution of the order parameter in reciprocal space. Meanwhile, consistent with the rather high transition temperatures, the energy gap scale has been reported to have an order of several hundred meV.[4–7,14,15]

Recently, apart from the above mentioned higher transitions, another anomaly was observed in the transport measurement[11] of the heavy rare-earth RTe₃ ($R =$ Dy, Ho, Er, and Tm) materials, which reveals that there exists another transition at a lower temperature. Then the notion is further confirmed by the following x-ray diffraction study.[11] A group of superlattice peaks, which develop below the transition, indicate that it has a CDW origin. The study reflects that a lattice modulation, which holds a wave vector along a^* axis, occurs perpendicular to the first one. Subsequent ARPES investigation of ErTe₃,[8] one of the heavy rare-earth tritellurides, which has two well-separated transitions at 267 and 155 K, observed multiple gap features at 10 K, which strengthened the notion that multiple CDW orders coexist in the system. The unmodulated spectral weight, which is located in the neighborhood of c^* axis in reciprocal space, was largely removed from the FS due to the first CDW gap formation, which is consistent with the previous ARPES studies on light rare-earth tritellurides. Furthermore, the intensity on the original FS in the vicinity of a^* axis is also clearly reduced, and then it is ascribed to the development of the second CDW order. The two energy gaps revealed by ARPES measurement are $\Delta_1 = 175$ meV and $\Delta_2 = 50$ meV, respectively.[8]

Optical spectroscopy is a powerful bulk-sensitive technique to detect the energy gaps in ordered state and yields a great wealth of information in CDW systems. The recent report of optical study on ErTe₃[16] suggests a partial gap formation roughly at 3000 cm^{-1} at low temperatures. Although the compound experiences two well-separated CDW transitions,[11] which are both believed to be located at rather high energy scales,[8] no information responsible for the second CDW transition was found in earlier optical measurement. Here, we

present an optical study on single crystalline ErTe$_3$. In sharp contrast to the previous assertion, the temperature-dependent spectra clearly reflect the development and evolution of both CDW orders. The first CDW transition has an energy gap $2\Delta_1 = 2770$ cm^{-1} ($\sim$343 meV) and the second one $2\Delta_2 = 890$ cm^{-1} ($\sim$110 meV) in the CDW state, both being in good agreement with the ARPES measurement.

II. EXPERIMENT AND RESULTS

The as-grown single crystalline samples of ErTe3, on which all the present measurements were performed, were grown by a self-flux method that was illustrated in detail in our earlier work.[15] The platelike single crystal with a shining golden surface (about 4×4 mm^2) is flexible and much convenient to cleave. We noticed that the sample is much more air- and moisture-sensitive than the light rare-earth element RTe$_3$ compounds.[15] After an exposure in air just a few days, the samples became soft and frail associated with a progressively darker surface. In order to avoid the deterioration, we have tried our best to diminish the samples' exposure time in air. Once the growth process came to the end and the single crystal was obtained, we carried out the measurements as soon as possible. Before each measurement process, a newly cleaved fresh surface is obtained. Meanwhile, each measurement was carried out several times to guarantee the repeatability and identity of the experimental results.

The temperature dependence of the in-plane (ac plane) dc conductivity is obtained by the standard four-probe method and plotted in Fig. 1. In agreement with previous studies,[11] two obvious anomalies near $T_{c1} = 267$ K and $T_{c2} = 150$ K are seen in the curve, and are ascribed to the two CDW transitions. No clear hysteresis is observed between cooling and warming processes, which is a clue that both transitions are second-order like.[8,11] The overall metallic behavior reveals that the FS is only partially affected across the two CDW transitions.[8]

The optical reflectivity measurement was bought out on a combination of Bruker IFS 113v and 80 v/s spectrometers in a frequency range from 40 to 40 000 cm^{-1}. An *in situ* gold and aluminium overcoating technique was used to get the reflectivity $R(\omega)$. Kramers-Kronig transformation of
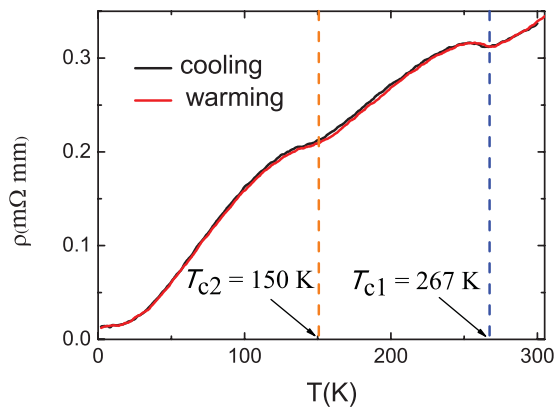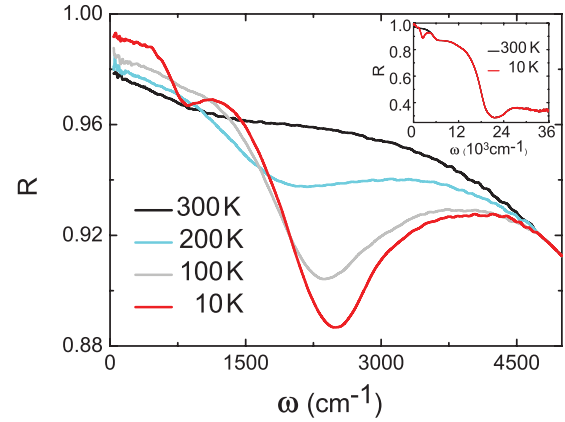

FIG. 2. (Color online) The reflectivity spectra $R(\omega)$ of ErTe$_3$ at varied temperatures in the range from 40 to 5000 cm^{-1}. Inset: the reflectivity spectra at two representative temperatures in an expanded range up to 36 000 cm^{-1}.

$R(\omega)$ is employed to get the real part of the conductivity spectra $\sigma_1(\omega)$. A Hagen-Rubens relation was used for the low-frequency extrapolation. In accordance with our earlier work,[15] a constant value of high frequency extrapolation was used up to 100 000 cm^{-1}, above which an ω^{-4} relation was employed.

The main panel of Fig. 2 focuses on the low-frequency range of the optical reflectivity spectra $R(\omega)$ up to 5000 cm^{-1}, while its inset displays the expanded range up to 36 000 cm^{-1} at two selected temperatures. The most significant character in $R(\omega)$ spectra is the development of a strong dip feature located in the midinfrared region upon cooling. We notice that there already exists a board suppression near 1500 cm^{-1} in the room-temperature spectrum. During the cooling process, the dip feature, which has been rather obvious at 200 K, becomes more and more dramatic. At the lowest temperature, it is rather pronounced. Furthermore, the center of the depletion shows a notable shift toward higher energies, roughly at 2500 cm^{-1} at 10 K. Additionally, at a lower energy scale, a second apparent suppression near 900 cm^{-1} is observed in $R(\omega)$ at 10 K. In opposition to the first one, it is much less pronounced and could not be clearly identified at the measurement temperatures above 100 K. It is worth noting that the suppressions are typical features of FS gap formation caused by density-wave instabilities.[15,17–19] As we shall elaborate below, these are the behaviors in reflectance corresponding with the two CDW orders respectively.

From the inset of Fig. 2, it could be concluded that all the spectra at varied temperatures coincide together roughly at 4700 cm^{-1}, above which the reflectance decreases slowly overall at first and displays an obvious broad kink near 6700 cm^{-1}. Different from the above mentioned two suppressions, the kink is already present at room temperature and exhibits no temperature dependence. As discussed in the next section, it should be ascribed to the interband transition. As frequency continues to proceed, the spectra drop sharply and form a well-defined reflectance edge (plasma edge), then merge with the background reflectance contributed from the interband transitions. The well-defined plasma edge, together with the rather high reflectivity in the extremely
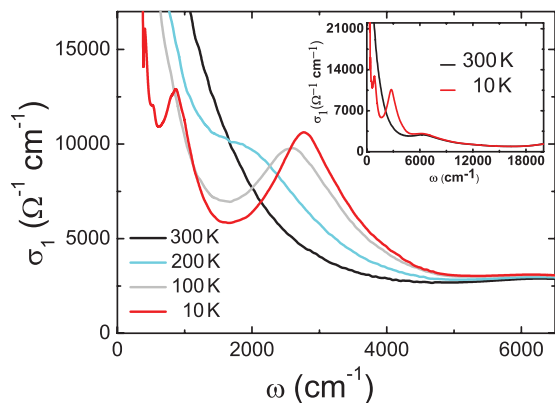

FIG. 1. (Color online) The temperature-dependent in-plane (ac plane) resistivity of single-crystal ErTe$_3$ for both cooling and warming processes. Two transitions emerge at $T_{c1} = 267$ K and $T_{c2} = 150$ K, respectively.

FIG. 3. (Color online) The temperature dependence of the real part of the conductivity $\sigma_1(\omega)$ up to 6500 cm^{-1}. The inset shows the spectra at 10 and 300 K over a broad frequency range.
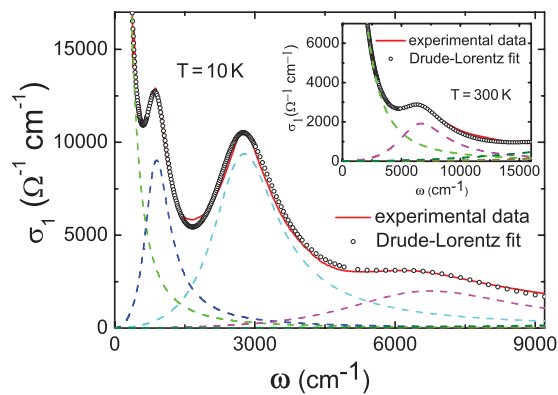

FIG. 4. (Color online) The experimental data of $\sigma_1(\omega)$ at 10 K and the Drude-Lorentz fit results. Each component of the fit displays at the bottom. Inset shows the corresponding results at 300 K.

low frequency region, demonstrate that the compound is a good metal even if it enters the CDW state. Below the two CDW energy scales, the reflectance increases monotonically when lowing temperatures, which is consistent with the dc resistivity measurement. It reinforces the metallic character of the material down to low temperatures, thus the FS is only partially gapped associated with the development of the CDW orders.

The real part of conductivity $\sigma_1(\omega)$ is displayed in Fig. 3 with its inset providing a global description in full range. A pronounced Drude component exists at all temperatures, confirming the metallic behavior. While in the CDW state, a notable midinfrared peak near 2800 cm^{-1} emerges in $\sigma_1(\omega)$ at 10 K. As temperature increases, the peak shifts slightly to lower energies and decreases in magnitude, tends to vanish at room-temperature spectra eventually. Furthermore, another similar peak feature at a lower energy scale appears only at 10 K. Corresponding with the two dip characters in $R(\omega)$, both peak features in $\sigma_1(\omega)$ indicate CDW-gap properties. Additionally, we note that the interband transition peak near 6700 cm^{-1} is also clearly seen at all temperatures.

III. DISCUSSION

To analyze the evolution of both the itinerant carrier resonance and the CDW gap excitations in a quantitative way, the $\sigma_1(\omega)$ spectra are fitted by the Drude-Lorentz model in the whole frequency range for all four temperatures:

$$\epsilon(\omega) = \epsilon_\infty - \frac{\omega_p^2}{\omega^2 + i\omega/\tau_D} + \sum_{i=1}^{N} \frac{S_i^2}{\omega_i^2 - \omega^2 - i\omega/\tau_i}. \quad (1)$$

Here, ϵ_∞ is the dielectric constant at high energy, the middle and last terms are the Drude and Lorentz components, respectively. A Drude term is employed to reproduce the metallic response and a selection of Lorentz components are used for the finite-frequency excitations, including the double peak gap features below the transition temperatures, an evident near-infrared peak centered roughly at 6700 cm^{-1}, and two high-energy ingredients above 25 000 cm^{-1} for inter-band transitions. The fit results at 10 K are presented in the main panel of Fig. 4 with its inset revealing the room-temperature

counterpart. In addition, the temperature dependence of the fit parameters, apart from the two high-energy constant interband transitions, are listed in Table I. In sharp contrast to the other terms of which the parameters experience remarkable changes at varied temperatures, the parameters of the third Lorentz component almost exhibit no temperature dependence. The central peak position is roughly pinned at 6700 cm^{-1} ($\sim$830 meV). The charge excitation is located at such a high-energy scale that it most likely originates from the interband transitions. In the following part, the discussions will be focused on the plasma frequencies, Drude scattering rate, and the two CDW gaps.

It is well known that the free-carrier resonance governs the Drude component behavior. The Drude spectral weight determines the plasma frequency ω_p, the square of which is proportional to the effective carrier density n/m^* (where m^* is the effective carrier mass). In addition, the width of the Drude peak is just the scattering rate $\gamma = 1/\tau$ (where τ is the average life time of free carriers). The plasma frequency $\omega_p = 47\,100$ cm^{-1} at 300 K reduces to 32 000 cm^{-1} at 10 K. Provided that the effective mass of free carriers remains the same at different temperatures, the area of the FS at 10 K will be 46% of that at room temperature, meaning that about half of the FS is gapped away from E_F. For the sake of verification

TABLE I. Temperature dependence of the plasma frequency ω_p and scattering rate $\gamma_D = 1/\tau_D$ of the Drude term, the resonance frequency ω_i, the width $\gamma_i = 1/\tau_i$ and the square root of the oscillator strength S_i of the Lorentz component (all entries in 10^3 cm^{-1}). One Drude mode is employed for all four measurement temperatures. Two Lorentz terms responsible for the CDW orders are added at low temperatures. The lowest energy interband transition is also displayed.

	ω_p	γ_D	ω_1	γ_1	S_1	ω_2	γ_2	S_2	ω_3	γ_3	S_3
300 K	47	1.00	...	...	...	...	...	...	6.7	5.0	24
200 K	41	0.55	...	...	...	2.0	2.1	28	6.7	4.8	23
100 K	39	0.41	...	...	...	2.6	2.1	31	6.7	4.7	23
10 K	32	0.15	0.89	0.65	19	2.8	1.7	31	6.7	4.6	23

and comparison, another approach is adopted to estimate the ungapped fraction of the FS:[16]

$$\Phi = \frac{\omega_p^2}{\omega_p^2 + \sum_{i=1}^{2} S_i^2}. \tag{2}$$

Where ω_p is the plasma frequency, S_i is the mode strength of the ith Lorentz peak. In analogy to the Drude component, the spectral weight $S_i^2/8$ is defined as the area under the Lorentzian curve. The summation applies to those Lorentz terms that come out only below the transitions. Apparently, this indicates that part of the spectral weight of the Drude component at high temperature is transferred to two Lorentz excitations in the CDW ordered state. The calculation gives a value $\Phi = 44\%$ at 10 K. Thus the above conclusion is well evidenced by the nearly same value. It is also worth noting that, in comparison with the relatively moderate change of the plasma frequency, the scattering rate experiences much stronger variations. The room-temperature value $\gamma = 1025$ cm^{-1} drops to 150 cm^{-1} at 10 K, which is a reduction of about 85%. It appears that the opening of partial CDW gaps removes the electrons near Fermi level that undergo stronger scattering.[15] Associated with the loss of scattering channels, the metallic behavior reveals an enhancement of the dc conductivity down to low temperatures.

Now, we focus on the discussion of the CDW properties. At the lowest temperature, $\sigma_1(\omega)$ spectra develop two typical gap features, the first one centered at 2770 cm^{-1} ($\sim$343 meV) and the second 890 cm^{-1} ($\sim$110 meV). It should be mentioned that the electrodynamics of broken symmetry states, such as superconductivity and density waves, has been well established and understood. For an s-wave superconductor at zero temperature, which holds the second case coherence factor, σ_1 equals zero below the single-particle gap, above which the spectra get a smooth rise. However, in the density-wave state, optical conductivity behaves much differently due to the first case coherence factor, which reaches a maximum at the gap frequency.[18,20,21] Based on these studies, the above mentioned central positions of the double peaks can be identified as the CDW energy gaps. Combined with the transition temperatures, we can get the ratio $2\Delta/k_B T_{CDW} = 14.9$ for the first CDW order and 8.5 for the second one. Both ratios are much higher than the weak-coupling theory predictions. It is worth pointing out that both CDW gap values obtained from the optical spectroscopy measurement match well with that extracted from ARPES experiments,[8] where a larger gap $\Delta_1 = 175$ meV and a smaller one $\Delta_2 = 50$ meV are obtained. Both values are almost identical with our results. Thus the present optical study is in good agreement with the ARPES measurement. In the previous optical report on the same compound,[16] only one gap feature near 3000 cm^{-1} was found. As we have mentioned above, the material is air and moisture sensitive. The surface degradation, if exposing in air for a bit longer time, may cause the discrepancy.

The evolution of the gap properties is apparent at varied temperatures. During the warming process, in $\sigma_1(\omega)$ spectra, the larger gap peak exhibits a sizable shift toward lower energies and decreases in magnitude, becomes invisible at room temperature eventually. On the other hand, the corresponding suppression in $R(\omega)$, as mentioned above, is clearly present at 300 K. It is most likely that the weak character due to
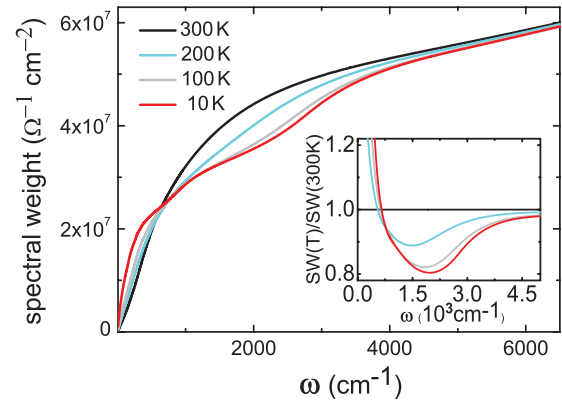

FIG. 5. (Color online) The temperature dependence of the spectral weight up to 6500 cm^{-1}. Inset: the normalized spectral weight SW(T)/SW(300K) up to 5000 cm^{-1}.

Lorentz excitation in the room-temperature spectra is covered by the high frequency tail of the large Drude component.[16] They match so well that we could not distinguish the charge excitation across the CDW gap from the itinerant carrier response. However, the transition temperature $T_{c1} = 267$ K in dc conductivity is well below the room temperature. The fact that CDW characters emerge above the transition supports the notion that in this two-dimensional compound, the fluctuation effect may be still functional. Such an effect is also confirmed by the observation, in an x-ray diffraction experiment,[11] of superlattice peaks with a broadened width well above T_{c1}. In addition, although the second transition temperature $T_{c2} = 150$ K is well above 100 K, the corresponding CDW gap excitation that exists in $\sigma_1(\omega)$ at 10 K could not be identified at 100 K. In contrast to the pronounced peak feature of the first CDW gap, the peak magnitude corresponding to the second CDW order is much weaker. Meanwhile, the peak position centered at 890 cm^{-1} is very close to the giant zero-energy excitations. So we believe that the disappearance of the second CDW peak in $\sigma_1(\omega)$ at 100 K has the same reason with the invisibility of the first one at 300 K.

To gain more insight into the band-structure variation accompanied with the CDW gap formations, a spectral weight analysis is present. The spectral weight as a function of frequency is plotted in Fig. 5 with the normalized one shown in the inset. In the extremely low-frequency range, consistent with the overall metallic behavior observed in dc resistivity measurements, the spectral weight increases monotonically with decreasing temperatures, due to the narrowing and rising of the Drude component. In the midinfrared frequency range, roughly between 700 cm^{-1} and 4500 cm^{-1}, the spectral weight at lower temperatures becomes smaller than that at higher ones. The redistribution clearly indicates the CDW gap formation. The inset of Fig. 5 shows that a notable minimum emerges in the normalized spectral weight in this area. At 10 K, a minimal value of 82% is reached at $\omega_{min} \approx 2000$ cm^{-1}. Consistent with the movement of the peak position in $\sigma_1(\omega)$, ω_{min} shifts remarkably to low frequency with increasing temperature, indicating that the CDW gaps tend to close. Above ω_{min}, the spectral weight differences between different temperatures diminish gradually, suggesting a spectral weight transfer from the low-frequency region below ω_{min} to the

high-frequency area above ω_{min}. Roughly above 9000 cm^{-1}, the curves for different temperatures merge together, indicating that the spectral weight is fully recovered. In the whole frequency range, the curve at 300 K is rather smooth, while subtle characters exist in the spectra at 10 K. There appears a slight downturn centered at 700 cm^{-1}, manifesting the opening of the smaller CDW gap. Additionally, another much striking suppression, verifying the formation of the larger gap, occurs in a broad frequency range from 1500 cm^{-1} to 3500 cm^{-1}.

It should be noted that, in contrast to the first CDW transition observed in the rare-earth based RTe$_3$ compounds,[13] which is pronounced almost in the whole lanthanides series,[11] the second CDW order is only reported in a fraction of the RTe$_3$ materials.[11,15] Apart from the prior reports of the second CDW transition brought out by transport[11] and ARPES measurement,[8] the present work undoubtedly confirmed the coexistence of multiple CDW transitions in ErTe$_3$, one of the heavy rare-earth tritelluride. Our earlier study on CeTe$_3$[15] has provided an optical evidence that multiple CDW orders also exist in the light rare-earth tritelluride. Therefore it is natural to ask whether or not the presence of the multiple CDW orders is a common feature in the rare-earth based RTe$_3$ compounds. Then, more systematic experimental investigations on various rare-earth based RTe$_3$ compounds would be necessary.

IV. CONCLUSIONS

To conclude, we have performed an optical investigation of the two CDW phase transitions of ErTe$_3$. The well-defined plasma frequency edge, which is present in the whole temperature range, and the rather high reflectivity in low-frequency range both demonstrate the well-behaved metallicity even in the CDW state. The depletion features in $R(\omega)$ and corresponding peak characters in $\sigma_1(\omega)$ both clearly reflect the development of the two CDW orders upon cooling. Two energy gaps, $2\Delta_1 = 343$ meV and $2\Delta_2 = 110$ meV at 10 K, are obtained via the Drude-Lorentz fit procedure. As the Drude component never disappears at low temperatures, the FS in the ordered state is only partially gapped. An optical estimation suggests that about half of the original FS is gapped away. The broad suppression feature in $R(\omega)$ at room temperature, which is yet above the first CDW transition, reflects that the fluctuation effect probably also plays an important role in this two-dimensional material.

[1]G. Grüner, *Density Waves in Solids* (Addison-Wesley, Reading, MA, 1994).

[2]E. DiMasi, M. C. Aronson, J. F. Mansfield, B. Foran, and S. Lee, Phys. Rev. B **52**, 14516 (1995).

[3]J. Laverock, S. B. Dugdale, Zs. Major, M. A. Alam, N. Ru, I. R. Fisher, G. Santi, and E. Bruno, Phys. Rev. B **71**, 085114 (2005).

[4]G. H. Gweon, J. D. Denlinger, J. A. Clack, J. W. Allen, C. G. Olson, E. D. DiMasi, M. C. Aronson, B. Foran, and S. Lee, Phys. Rev. Lett. **81**, 886 (1998).

[5]V. Brouet, W. L. Yang, X. J. Zhou, Z. Hussain, N. Ru, K. Y. Shin, I. R. Fisher, and Z. X. Shen, Phys. Rev. Lett. **93**, 126405 (2004).

[6]H. Komoda, T. Sato, S. Souma, T. Takahashi, Y. Ito, and K. Suzuki, Phys. Rev. B **70**, 195101 (2004).

[7]V. Brouet, W. L. Yang, X. J. Zhou, Z. Hussain, R. G. Moore, R. He, D. H. Lu, Z. X. Shen, J. Laverock, S. B. Dugdale, N. Ru, and I. R. Fisher, Phys. Rev. B **77**, 235104 (2008).

[8]R. G. Moore, V. Brouet, R. He, D. H. Lu, N. Ru, J. H. Chu, I. R. Fisher, and Z. X. Shen, Phys. Rev. B **81**, 073102 (2010).

[9]B. K. Norling and H. Steinfink, Inorg. Chem. **5**, 1488 (1966).

[10]E. DiMasi, B. Foran, M. C. Aronson, and S. Lee, Chem. Mater. **6**, 1867 (1994).

[11]N. Ru, C. L. Condron, G. Y. Margulis, K. Y. Shin, J. Laverock, S. B. Dugdale, M. F. Toney, and I. R. Fisher, Phys. Rev. B **77**, 035114 (2008).

[12]A. Sacchetti, C. L. Condron, S. N. Gvasaliya, F. Pfuner, M. Lavagnini, M. Baldini, M. F. Toney, M. Merlini, M. Hanfland, J. Mesot, J. H. Chu, I. R. Fisher, P. Postorino, and L. Degiorgi, Phys. Rev. B **79**, 201101(R) (2009).

[13]N. Ru and I. R. Fisher, Phys. Rev. B **73**, 033101 (2006).

[14]A. Sacchetti, L. Degiorgi, T. Giamarchi, N. Ru, and I. R. Fisher, Phys. Rev. B **74**, 125115 (2006).

[15]B. F. Hu, P. Zheng, R. H. Yuan, T. Dong, B. Cheng, Z. G. Chen, and N. L. Wang, Phys. Rev. B **83**, 155113 (2011).

[16]F. Pfuner, P. Lerch, J. H. Chu, H. H. Kuo, I. R. Fisher, and L. Degiorgi, Phys. Rev. B **81**, 195110 (2010).

[17]W. Z. Hu, G. Li, J. Yan, H. H. Wen, G. Wu, X. H. Chen, and N. L. Wang, Phys. Rev. B **76**, 045103 (2007).

[18]W. Z. Hu, J. Dong, G. Li, Z. Li, P. Zheng, G. F. Chen, J. L. Luo, and N. L. Wang, Phys. Rev. Lett. **101**, 257005 (2008).

[19]W. Z. Hu, G. Li, P. Zheng, G. F. Chen, J. L. Luo, and N. L. Wang, Phys. Rev. B **80**, 100507(R) (2009).

[20]M. Dressel, and G. Grüner, *Electrodynamics of Solids* (Cambridge, Reading, 2002).

[21]L. Degiorgi, M. Dressel, A. Schwartz, B. Alavi, and G. Grüner, Phys. Rev. Lett. **76**, 3838 (1996).